https://ntrs.nasa.gov/search.jsp?R=19650023525 2018-07-23T22:56:11+00:00Z

NGR-47-004-006

LAMINAR FLOW PAST A SHPERE AT HIGH MACH NUMBER[1]

By

R. T. Davis[2] and W. J. Chyu[3]

GPO PRICE $ ______

CSFTI PRICE(S) $ ______

Hard copy (HC) 2.00

Microfiche (MF) .50

ff 653 July 65

N65-33126 (ACCESSION NUMBER)

27 (PAGES)

CR 64595 (NASA CR OR TMX OR AD NUMBER)

1 (THRU)

(CODE)

01 (CATEGORY)

FACILITY FORM

---

[1]This research was supported in part by NASA

[2]Assistant Professor, Engineering Mechanics Department, Virginia Polytechnic Institute

[3]Graduate Student, Engineering Mechanics Department, Virginia Polytechnic Institute

1. Introduction

The high speed flow of a compressible fluid over a blunt body at moderate to low Reynolds numbers has attracted considerable attention due to its application to re-entry problems. The flow regime where the Reynolds number is high enough for boundary-layer theory to apply can be handled without too much difficulty. This is done by obtaining a numerical solution to the inviscid flow equations describing the flow outside the boundary-layer and using this solution to obtain the pressure distribution on the body surface. One can then use this pressure distribution to solve the boundary-layer equations by one of several methods available such as those of Flügge-Lotz and Blottner (1962), Smith and Clutter (1963), and Davis and Flügge-Lotz (1964) (The last method is actually a modification of the method of Flügge-Lotz and Blottner.) Boundary-layer calculations have been made for several flow cases by using the above methods. In particular one is referred to the hypersonic blunt body solutions by Davis and Flügge-Lotz (1964).

As one encounters lower Reynolds numbers one must contend with the fact that one cannot expect the first-order boundary-layer equations to give reasonable results. This can be corrected at the high Reynolds number end by solving the so-called second-order boundary-layer equations. This has also been done by Davis and Flügge-Lotz (1964). This, however, becomes quite cumbersome and requires a considerable amount of computing time. If one needs to go to third-order boundary-layer theory to get sufficient accuracy one would find the situation even more difficult. One of the difficulties encountered is the problem of calculating the flow due to displacement thickness. This requires a direct solution for the inviscid flow past a body consisting of the original body thickened by the displacement thickness. Davis and Flügge-Lotz (1964) approximated this flow by shifting and expanding the original body surface. Hoffman (1964) has approached the problem in a more exact manner by using the method of integral relations to calculate the flow field. Neither method is entirely satisfactory, the first because of inaccuracy and the second because of computational difficulties. Another difficulty with higher order boundary-layer theory is the fact that at moderate Reynolds numbers the boundary-layer begins to spread into the entire shock layer preventing one from clearly distinguishing separate inviscid and viscous regions [see Kao(1964)] and therefore limiting boundary-layer theory to higher Reynolds numbers than one might expect.

For the reasons above one is lead to the idea of trying to solve the complete Navier-Stokes equations or a simplification to them which is valid in the whole shock-layer. Davis and Flügge-Lotz (1964) have suggested such a simplification and a method for solving their simplified equations. The purpose of this paper is to present the results of an investigation which uses the method suggested by Davis and Flügge-Lotz (1964).

For simplicity we will consider the constant density flow past a sphere. There are several reasons for this. First, an exact inviscid solution due to Lighthill (1957) is available for comparison for the inviscid part of the flow field in the high Reynolds number flows. Second, the constant density model will retain all of the essential features for the numerical procedure for the solution of the flow of the more complicated compressible fluid. Once the constant density case has been solved the extension to the compressible case is direct with no complications arising due to theory. For simplicity we will also assume that the shock is a discontinuity even in the low Reynolds number cases. This is again a simplification which can be removed [see Cheng (1963)].

In order to start the numerical procedure one must have a solution which is valid near the stagnation point. The ideal method for finding this solution is to use the series truncation method developed by Van Dyke and co-workers. In particular the truncated series method used by Kao (1964) in the compressible viscous flow past a sphere is useful. The truncated series results should be particularly good since the form of the truncation is taken to be the same as the form of the inviscid constant density solution . These results are also used for comparison with the numerical finite - difference results.

For the purpose of comparison with the high Reynolds number cases the first-order boundary-layer equations are also solved for the constant density flow. In this case Lighthill's (1957) constant density solution is used for determining the surface pressure distribution.

2. Formulation of the problem

2.1 Co-ordinate system

Consider laminar hypersonic flow of a viscous fluid past the sphere of radius a* shown in figure 1. For simplicity we will assume that the free stream Mach number M_∞ is infinite and that the density ρ_s^* and viscosity μ_s^* in the flow field behind the shock are constants given by their values immediately behind the normal shock. The velocity components u* and v* are tangent and normal to the body surface respectively. The coordinate n* is measured normal to the body surface and the angle ϕ is measured from the stagnation-point to the radius vector.

2.2 Dimensionless quantities

For simplicity the following dimensionless quantities are introduced. These quantities are of order one in the boundary-layer region near the surface of the sphere.

$N = \frac{n^*}{\tau a^*}$, boundary-layer normal coordinate (2.1a)

$a = \frac{a^*}{a^*} = 1$, nose radius (2.1b)

$u = \frac{u^*}{U_\infty^*}$, the velocity component parallel to the body surface (2.1c)

$p = \frac{p^*}{\rho_\infty^* U_\infty^{*2}}$, the pressure (2.1d)

$\rho_s = \frac{\rho_s^*}{\rho_\infty^*} = 6$, the density behind the shock for $M_\infty = \infty$ (2.1e)

$(\tau_f)_w = \frac{(\tau_f^*)_w \sqrt{Re_s}}{\rho_\infty^* U_\infty^{*2}} = \frac{\partial u}{\partial N}$, shear stress at the body surface (2.1f)

$$Re_s = \frac{U_\infty^* a^* \rho_\infty^*}{\tau_s^*} \quad \text{, shock Reynolds number} \tag{2.1g}$$

The quantity τ used in the above relations is defined by

$$\tau = \frac{1}{\sqrt{Re_s}} \tag{2.1h}$$

2.3 Assumptions

We will assume that the constant density model is applicable. This will be true near the stagnation-point for a nearly insulated body. We will further assume that the no-slip conditions apply at the body surface. These conditions can be modified to take care of slip with little difficulty [see Street (1950)]. We will also assume that the bow shock wave is a discontinuity even though at low Reynolds numbers this is not true. This restriction can be removed in a manner similar to that of Cheng (1963). All of these restrictions are imposed to allow attention to be focused on the numerical procedure. The restrictions of constant density, no-slip etc., can be removed with little change in the method of solution. These more general calculations which conform more closely with the real situation are presently being made.

The last assumption is that the bow shock wave angle is the same as the body angle for a given value of ϕ. This is similar to assuming a spherical shock except that the distance between the body and the shock is allowed to grow. Since the shock is spherical in the inviscid case this assumption is very good for high Reynolds numbers. On the basis of the numerical calculations we will see that this is not a bad assumption even at low Reynolds numbers. We have tried to build up the shock wave in the viscous case as the computations proceed downstream, however this has lead to instabilities in the numerical procedure. This point is presently under study and an attempt is being made to impose the shock conditions in such a way that instabilities do not occur. This difficulty must be overcome before other body shapes are considered along with a compressible fluid.

Assumptions similar to some of those made above (i.e. constant density etc.) have been made by Probstein and Kemp (1960), Oguchi (1958), and Hoshizaki (1959) in considering the viscous flow past a sphere.

2.4 Governing Equations and Boundary Conditions

Introducing the dimensionless quantities (2.1a) - (2.1g) into the full Navier-Stokes equations and neglecting all terms of higher order in Reynolds number than second that will appear in both the boundary-layer region near the body and also in the inviscid region outside this layer we can obtain a set of equations similar to those given by Davis and Flügge-Lotz (1964). [See their paper for a discussion of this approximation.] Upon making the constant density approximation we obtain the following set of partial differential equations and boundary conditions.

Continuity*

$$[\{(1+\tau N)\sin\phi\}u]_\phi+[(1+\tau N)\{(1+\tau N)\sin\phi\}v]_N=0 \tag{2.2a}$$

ϕ-Momentum

$$\rho_s\left(\frac{uu_\phi}{1+\tau N}+vu_N+\frac{\tau}{1+\tau N}uv\right)+\frac{P_\phi}{1+\tau N}=u_{NN}+\frac{2\tau}{1+\tau N}u_N \tag{2.2b}$$

N-Momentum

$$\rho_s\left(\frac{\tau uv_\phi}{1+\tau N}+\tau vv_N-\frac{u^2}{1+\tau N}\right)+\frac{1}{\tau}P_N=0 \tag{2.2c}$$

Surface Conditions

$$u,\ v=0 \text{ at } N=0 \tag{2.2d}$$

*Subscripts s denote conditions behind the normal shock and subscripts ϕ and N denote differentiation.

Shock Conditions (Spherical, $M_\infty = \infty$)

$$P_s = \frac{2}{\gamma+1} - \frac{2}{\gamma+1}\sin^2\phi \qquad (2.2e)$$

$$u_s = \sin\phi \qquad (2.2f)$$

$$v_s = -\frac{1}{\tau}\frac{(\gamma-1)}{(\gamma+1)}\cos\phi \qquad (2.2g)$$

The position of the shock will be located by the requirement that the conditions (2.2e) - (2.2g) above be satisfied. In addition total mass conservation between the body and the shock is checked by the condition that

$$(1+\tau N_s)^2 \sin\phi = 2\tau \rho_s \int_0^{N_s} u(1+\tau N)\,dN \qquad (2.2h)$$

The value of N_s at which this condition is satisfied can also be used to determine the shock position.

3. Methods of Solution of the Governing Equation

3.1 Series truncation method

In order to start the numerical finite-difference method it is necessary to have an accurate solution for the flow near the stagnation-point. The series truncation method developed and applied by Van Dyke and co-workers is ideal for doing this. In the constant density flow past a sphere it is obvious that the form that one should take for the truncation is the form of the constant density inviscid solution of Lighthill (1957). This should be particularly accurate in the high Reynolds number range when the boundary-layer is thin and the shock is nearly spherical. The form of the truncation used by Kao (1964) for the compressible case is exactly the same as the form which will be used here. Probstein and Kemp (1960) and other authors have made similar truncations in solving the same problem of constant density flow past a sphere.

Assume

$$P(N,\phi) = P_1(N) + P_2(N)\sin^2\phi + \cdots \qquad (3.1a)$$

$$u(N,\phi) = u_1(N)\sin\phi + \cdots \qquad (3.1b)$$

$$v(N,\phi) = - v_1(N) \cos \phi + \cdots \tag{3.1c}$$

Substituting these expressions into the continuity and momentum equations (2.2a - c) and collecting terms we obtain the following set of ordinary differential equations,

$$(1+\tau N)v_{1N} - 2(u_1 - \tau v_1) = 0 \tag{3.2a}$$

$$u_{1NN} + (\rho_s v_1 + \frac{2\tau}{1+\tau N}) u_{1N} - \rho_s \frac{u_1^2}{1+\tau N} + \rho_s \frac{\tau u_1 v_1}{1+\tau N} - \frac{2P_2}{1+\tau N} = 0 \tag{3.2b}$$

$$P_{2N} - \tau \rho_s (\frac{u_1^2}{1+\tau N} + \tau v_1 v_{1N} - \frac{\tau u_1 v_1}{1+\tau N}) = 0 \tag{3.2c}$$

$$P_{1N} - \tau^2 \rho_s v_1 v_{1N} = 0 \tag{3.2d}$$

The corresponding surface and shock conditions are:

<u>At the body,</u>

$$u_1 \text{ , } v_1 = 0 \text{ at } N = 0 \tag{3.2e}$$

<u>At the shock (Spherical, $M_\infty = \infty$),</u>

$$v_{1s} = \frac{1}{\tau} \frac{\gamma-1}{\gamma+1} \tag{3.2f}$$

$$u_{1s} = 1 \tag{3.2g}$$

$$P_{2s} = - \frac{2}{\gamma+1} \tag{3.2h}$$

$$P_{1s} = \frac{2}{\gamma+1} \tag{3.2i}$$

Finally, conservation of mass requires that

$$(1+\tau N_s)^2 = 2\tau\rho_s \int_0^{N_s} u_1(1+\tau N)dN \tag{3.2j}$$

It should be noted that the first three differential equations (3.2a-c) do not involve P_1 and can therefore be solved independent of P_1. After the solution is obtained, P_1 can be determined from equation (3.2d).

The set of equations (3.2a-c) is fourth order. Only two boundary conditions are given at the body surface (N=0). The method of solution is to guess values for P_2 and u_{1N} at the body surface and then integrate numerically starting from the body surface. Good initial guesses can be made for P_2 and u_{1N} on the basis of boundary-layer theory. Lighthill's (1957) inviscid constant density solution along with one term of the Blasius series expansion for the boundary-layer equations near the stagnation-point provide a fairly good initial guess even in the low Reynolds number cases. The integration is carried out until the shock condition on u_1 is satisfied. Values of v_1 and P_2 will then be determined. Interpolation using Newton's method will allow the shock conditions on v_1 and P_2 to be satisfied after a few trys. It was found that mass conservation equation (3.2j) was satisfied to sufficient accuracy.

The numerical scheme used was the Runge - Kutta - Gill method on an I. B. M. 7040 electronic digital computer. Each integration required less than one minute computing time and sufficient accuracy was assured by halving the step size until no change in the results was noted in the first four decimal places. The numerical results were carried out for values of Re_s of 900,100, and 49 (τ = 1/30,1/10, and 1/7). The results of these computations will be discussed later along with the results from the finite-difference method. The results are in agreement with those of Probstein and Kemp (1960).

3.2 Finite-Difference Method

The main simplification is to reduce the Navier-Stokes equations governing the fluid motion to a set of parabolic partial differential equations so that backward influence is eliminated, and so that integration can be performed by starting from the stagnation-point and integrating downstream along the body surface. The first step in doing this is to use the simplified form of the Navier-Stokes equations (2.2a-c) which retain only terms up to second-order for large Reynolds number. The significance of these equations as far as numerical integration is concerned has been discussed by Davis and Flügge-Lotz (1964). [A similar set of equations has been used by Cheng (1963).]

The method of solution used is similar to the implicit finite-difference method developed by Flügge-Lotz and Blottner (1962) for solving the boundary-layer equations. For details of the method one is referred to Flügge-Lotz and Blottner (1962) and Davis and Flügge-Lotz (1964).

A three point backward difference scheme in the ϕ direction is used for high accuracy in evaluating the derivatives in the ϕ direction. [See Davis and Flügge-Lotz (1964)] In the discussion that follows no mention will be made of the differences in the N direction since the method for handling these is exactly the same as the method used by Flügge-Lotz and Blottner (1962) or Davis and Flügge-Lotz (1964).

The flow field between the body and the shock is overlaid with a grid of lines parallel to the N and ϕ coordinate lines respectively. It is assumed that the spacing ($\Delta\phi$ and ΔN) between the grid lines is constant. Grid lines normal to the body surface, i.e. lines of constant ϕ are denoted with a subscript m. It is assumed that flow quantities are known initially [from the series truncation solution] along the grid lines $\phi = \phi_m$ and $\phi = \phi_{m-1}$. The unknown quantities are then at $\phi = \phi_{m+1} = \phi_m + \Delta\phi$. A difference equation can then be obtained from the ϕ momentum equation at the point $\phi = \phi_{m+1}$ in the same manner as that used by Davis and Flügge-Lotz (1964) on the boundary-layer equations. This difference equation is linearized by replacing nonlinear quantities like

$v_{m+1}(\frac{\partial u}{\partial N})_{m+1}$ by $(2v_m - v_{m-1})(\frac{\partial u}{\partial N})_{m+1}$. By linearizing in this manner we eliminate the unknown quantitiy v_{m+1} from the momentum equation. The only two remaining unknowns in that equation are then u and P. We further simplify the equation by eliminating $P_{\phi m+1}$ by the relation

$$P_{\phi m+1} = 2P_{\phi m} - P_{\phi m-1} + O(\Delta\phi^2) \tag{3.3}$$

By writing $(\frac{\partial u}{\partial N})_{m+1}$, $(\frac{\partial^2 u}{\partial N^2})_{m+1}$ etc. in difference form in the N direction we now have an equation for the determination of u only at the station m+1. This involves the solution of simultaneous algebraic equations, however the method of solution is simple and direct [See Richtmyer (1957) and Flügge-Lotz and Blottner (1962)].

After u_{m+1} has been determined at all points across the shock layer v_{m+1} can be determined from the continuity equation by numerical integration.

This is given by

$$v = -\left(\frac{1}{(1+\tau N)^2 \sin\phi}\right) \int_0^N [\{(1+\tau N)\sin\phi\}u]_\phi \, dn \tag{3.4}$$

where all terms on the right hand side are known and v_{m+1} can then be determined by integrating to the value of N corresponding to the grid point of interest. The derivative inside the integral is evaluated by using a three point backward difference quotient, and the integration is then performed by using the trapazoidal or some other integration formula.

Now that v_{m+1} has been determined at all points across the shock layer at station m+1, we may determine P_{m+1}. This is done in the same manner as was used for v_{m+1} but by integrating the N-momentum equation. This gives

$$P = P_w + \tau\rho_s \int_0^N \left[\frac{u^2}{1+\tau N} - \frac{\tau u v_\phi}{1+\tau N} - \tau v v_{1N}\right] dN \tag{3.5}$$

where P_w is the pressure at the body surface, and is determined by making the above equation satisfy the correct condition on pressure at the shock. It was found that near the stagnation-point, the inclusion of the second two terms of the integrand in equation (3.5) led to numerical instabilities. For this reason they were neglected in the finite-difference calculations but were then included in a second iteration in determining the pressure. This assumption is consistent with thin shock-layer theory and gives excellent agreement with the series truncation results. The adequacy of equation (3.3) in determining the pressure gradient at the station m+1 was also checked by iteration at station m+1, and it was found that there was very little change in the results for the pressure distribution.

Using the solution obtained in the manner above as a first step it may be possible to build up a more exact solution to the Navier-Stokes equations by an iteration procedure. This possibility is being considered at the present time in addition to the extension of the numerical method to a compressible fluid.

4. Results

The results for the solutions using both the series truncation method and the finite-difference method are shown in figures 2-5.

Figure 2 indicates that at high Reynolds number the shock is spherical as Lighthill's (1957) inviscid solution indicates. Even in the low Reynolds number cases, however, the deviation from a spherical shock is small. This gives an indication that the assumption of a spherical shock is a good one.

Figures 3a-c show the u component of velocity between the body and the shock. One can see from the figures that the results from the series truncation method and the finite-difference method are in close agreement for small ϕ . This is what one would expect since only one term is used in the series truncation method. One also notices that in going to the higher Reynolds numbers one has the clear indication of the formation of a boundary-layer. However, even in the case of Reynolds number of 100 the indication is that the viscous effects extend over most of the shock layer. Figure 3c (Re_s = 900) has a comparison with Lighthill's (1957) constant density inviscid solution. In the inviscid part of the flow field one sees that there is good agreement between the two solutions. If one included the effect of displacement thickness to obtain the inviscid solution, one would find even better agreement.

Figures 4a-d show the variation of skin friction over the sphere. As one would expect the truncated series method and the finite-difference agree well only near the stagnation-point. Figure 4d shows the results from the finite-difference method for the full shock-layer as compared with the finite-difference method used on the boundary-layer equations. One sees that the agreement is good at high Reynolds numbers. The boundary-layer solution was obtained by using Lighthill's (1957) constant density solution to obtain the pressure distribution on the sphere.

Finally, figures 5a-d show pressure distributions for the flow past the sphere. Figures 5a-c show pressure distributions across the shock-layer. The agreement between the truncated series method and the finite-difference method is excellent for all positions in the shock layer. The fact that the pressure agreement between the two methods is so good is due to the fact that the pressure distribution across the viscous region (boundary-layer) is essentially constant. This means the since the form of the truncation was taken to be the same as the constant density inviscid flow, one would expect good agreement in the pressures. Figure 5d shows the surface pressure distribution on the sphere. The difference between the finite-difference method and truncated series method is so slight that it cannot be detected on the plot. It is noticed that the pressure distribution is going towards Lighthill's constant density solution as Reynolds number increases. This is as one would expect since Lighthill's pressure distribution should be valid for Reynolds number infinity.

5. Conclusions

It has been demonstrated that it is possible to integrate numerically a set of equations valid in the entire shock layer which are an approximation to the Navier-Stokes equations for high Reynolds number. These equations are integrated by starting at the stagnation-point and integrating downstream with the use of an implicit finite-difference method. The case considered was for the constant density viscous flow past a sphere, however the method for handling the compressible case is completely analogous. The results obtained agree with those obtained from the series truncation solution and also with the inviscid constant density solution of Lighthill (1957) when the Reynolds number is high enough. Effects such as shock structure and slip have not been included, however they can easily be considered since the numerical procedure for solving the governing equations is now clear.

In the future the method can be used for determining solutions to problems such as the flow far downstream on a hyperboloid in compressible supersonic flow. From the boundary-layer point of view it is not clear what the solution is in the region where the entropy-layer and boundary-layer merge. The method used here is not concerned with these difficulties since the entire shock layer is treated at once.

REFERENCES

Cheng, H. K. 1963 "The Blunt-Body Problem in Hypersonic Flow at Low Reynolds Number." Cornell Aero. Lab. Rep. no. AF-1285-A-10.

Davis, R. T. and I. Flügge-Lotz 1964 "Second-Order Boundary-Layer Effects in Hypersonic Flow Past Axisymmetric Blunt Bodies." J. Fluid Mech. vol. 20, part 4.

Flügge-Lotz, I. and F. G. Blottner 1962 "Computation of the Compressible Laminar Boundary-Layer Flow Including Displacement-Thickness Interaction Using Finite-Difference Methods." Div. Engng. Mech., Stanford Univ., Tech Rep. no. 131. (Abbreviated version published in J. Mechanique, 2, pp. 397-423.)

Hoffman, G. H. 1964 "Solution of the Inviscid Flow Due to Displacement by the Method of Integral Relations." Lockheed Missiles and Space Company, Tech Rep. no. H-64-017.

Hoshizaki, H. 1959 "Shock-Generated Vorticity Effects at Low Reynolds Number." Lockheed Aircraft Corp., Missiles and Space Div. Rep., LMSD-48381 vol. 1, pp. 9-43.

Kao, H. C. 1964 "Hypersonic Viscous Flow Near the Stagnation Streamline of a Blunt Body: I. A Test of Local Similarity." AIAA Journal, vol. 2, no. 11.

Lighthill, M. J. 1957 "Dynamics of a Dissociating Gas, Part I, Equilibrium Flow." J. Fluid Mech. 2, pp. 1-32.

Oguchi, H. 1958 "Flow Near the Forward Stagnation Point of a Blunt Body of Revolution." Journal of the Aero/Space Sciences, vol. 25, no. 12, pp. 789-790.

Probstein, R. F. and N. H. Kemp 1960 "Viscous Aerodynamic Characteristics in Hypersonic Rarefied Gas Flow." Journal of Aero/Space Sciences, vol. 27, no. 3, pp. 174-192.

Smith, A. M. O. and D. W. Clutter 1963 "Solution of the Incompressible Laminar Boundary-Layer Equations." AIAA Journal, vol. 1, no. 9.

Street, R. E. 1960 "A Study of Boundary Conditions in Slip-Flow Aerodynamics." Rarefied Gas Dynamics (F. M. Devienne, ed.), pp. 276-92, Pergamon Press, London.

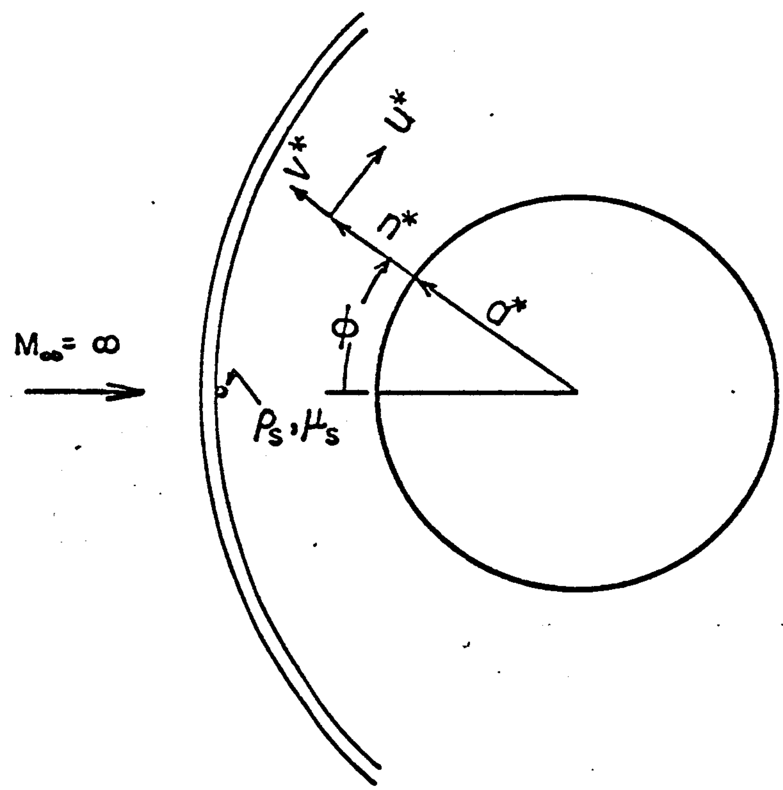

Figure 1 Co-ordinate System

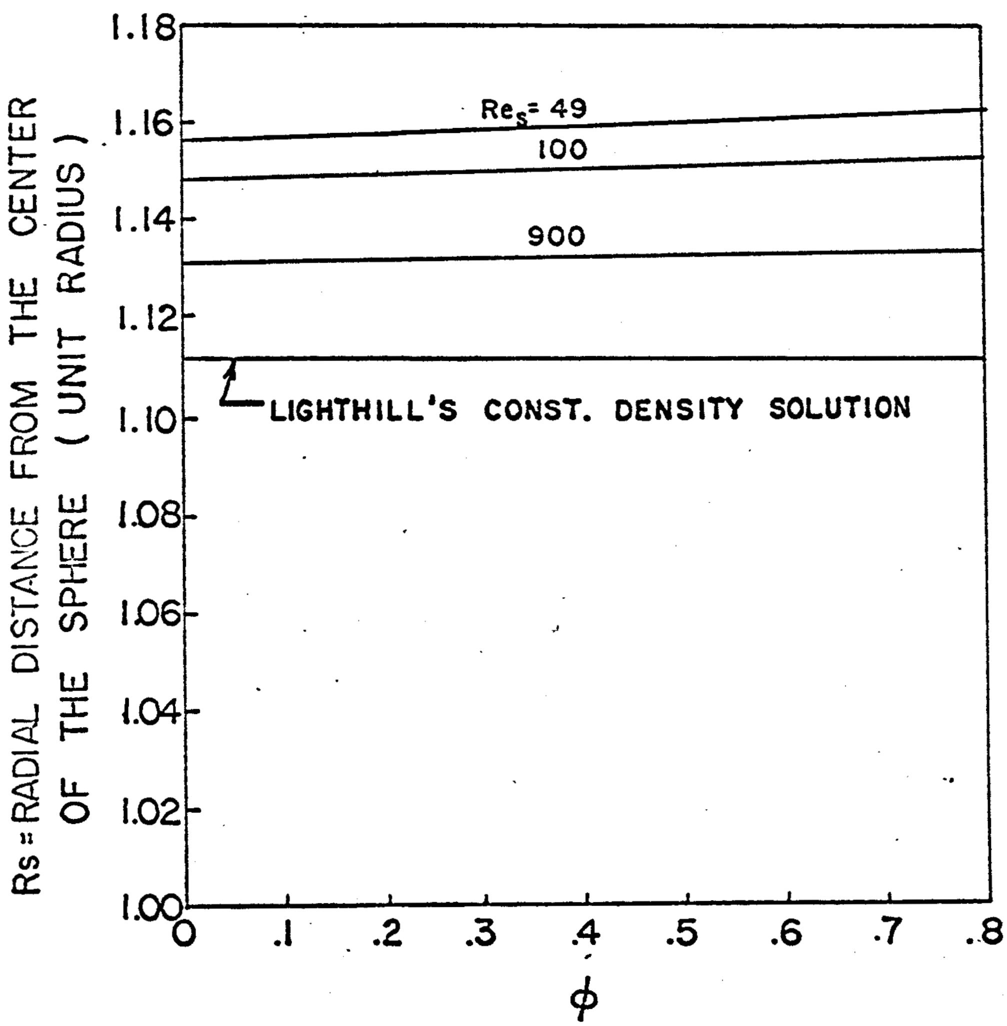

Figure 2 Radial Distance to the Shock at Various Reynolds Numbers

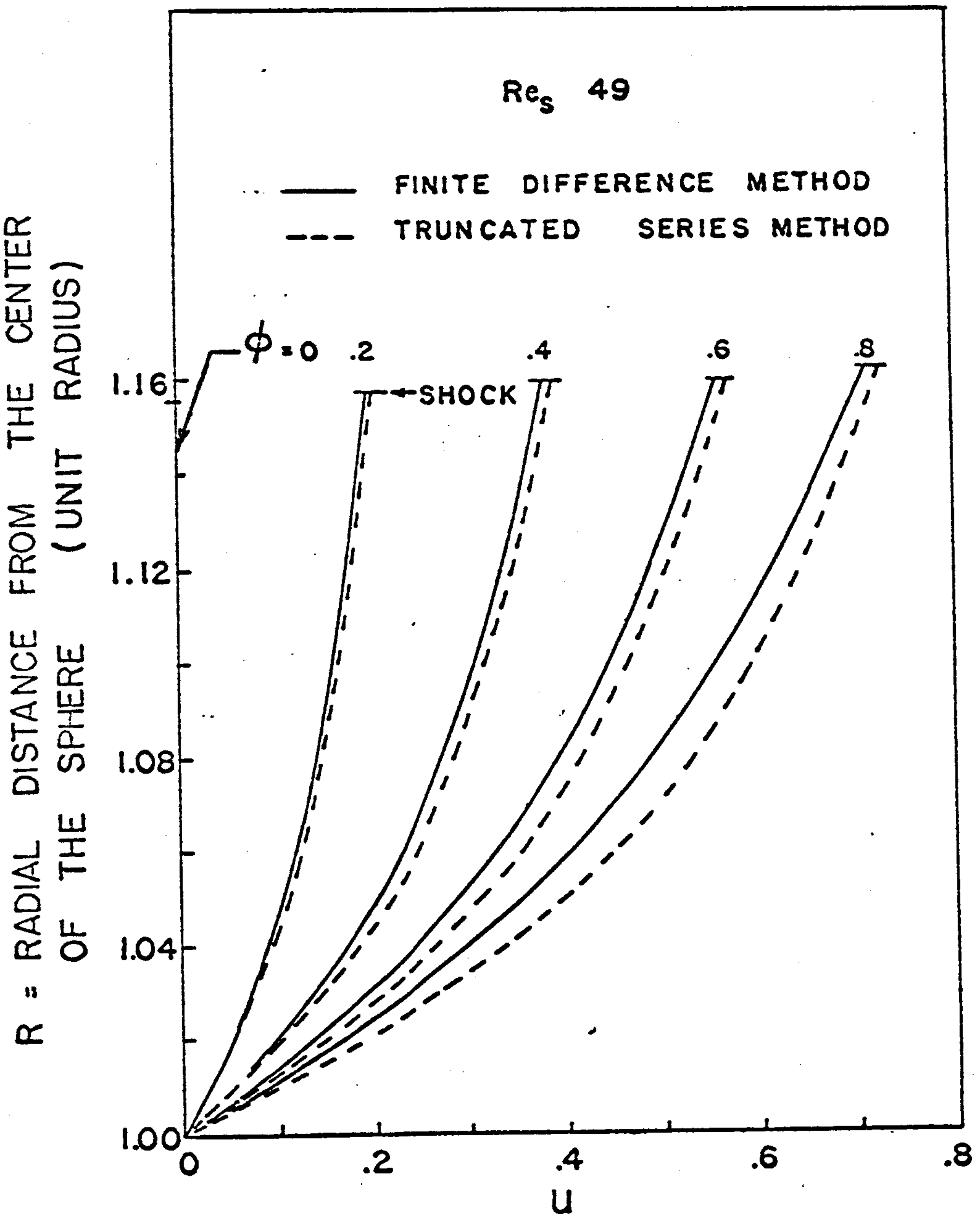

Figure 3a Velocity Distribution in the Shock-Layer for $Re_s = 49$

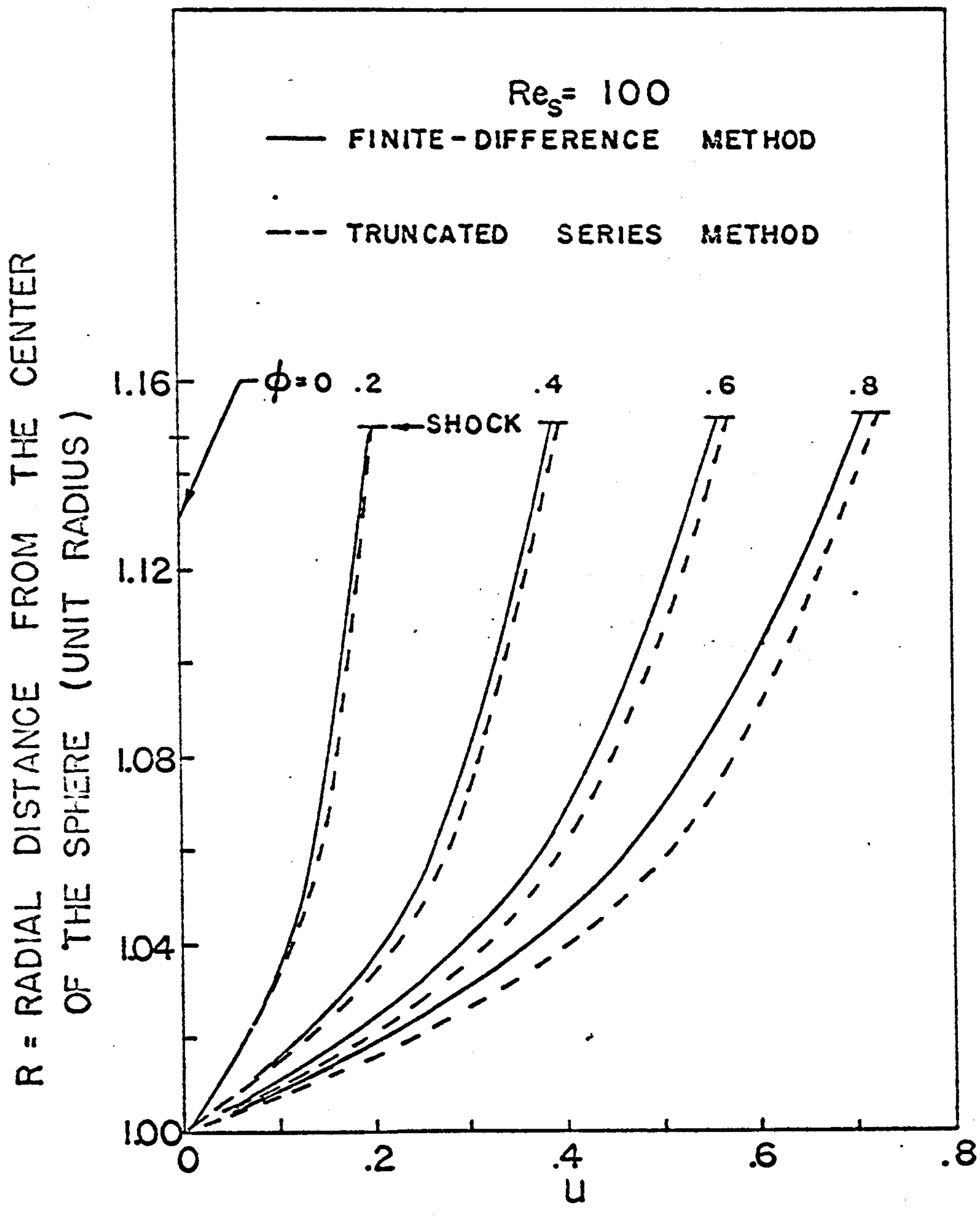

Figure 3b Velocity Distribution in the Shock-Layer for Re$_s$ = 100

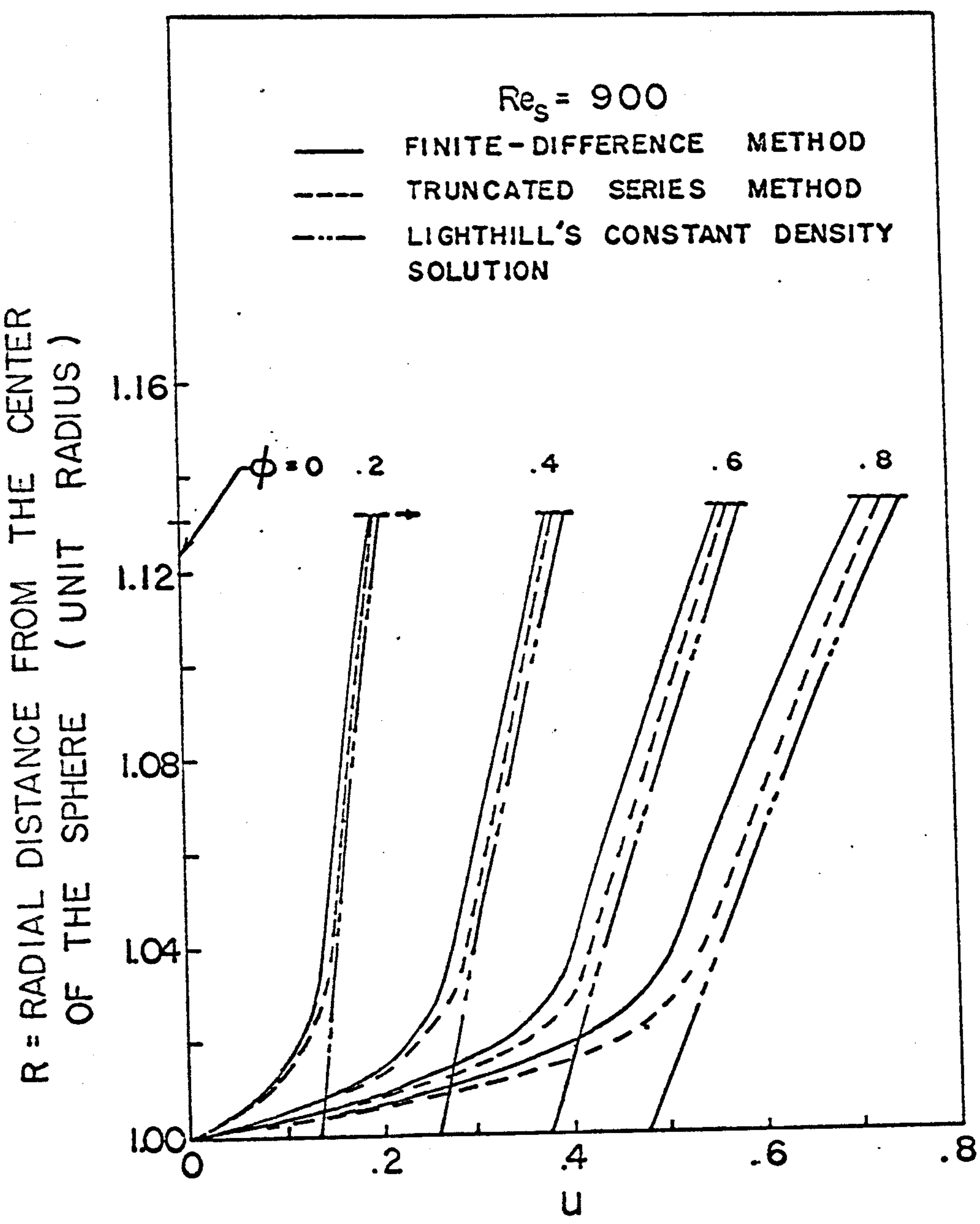

Figure 3c Velocity Distribution in the Shock-layer for $Re_s = 900$

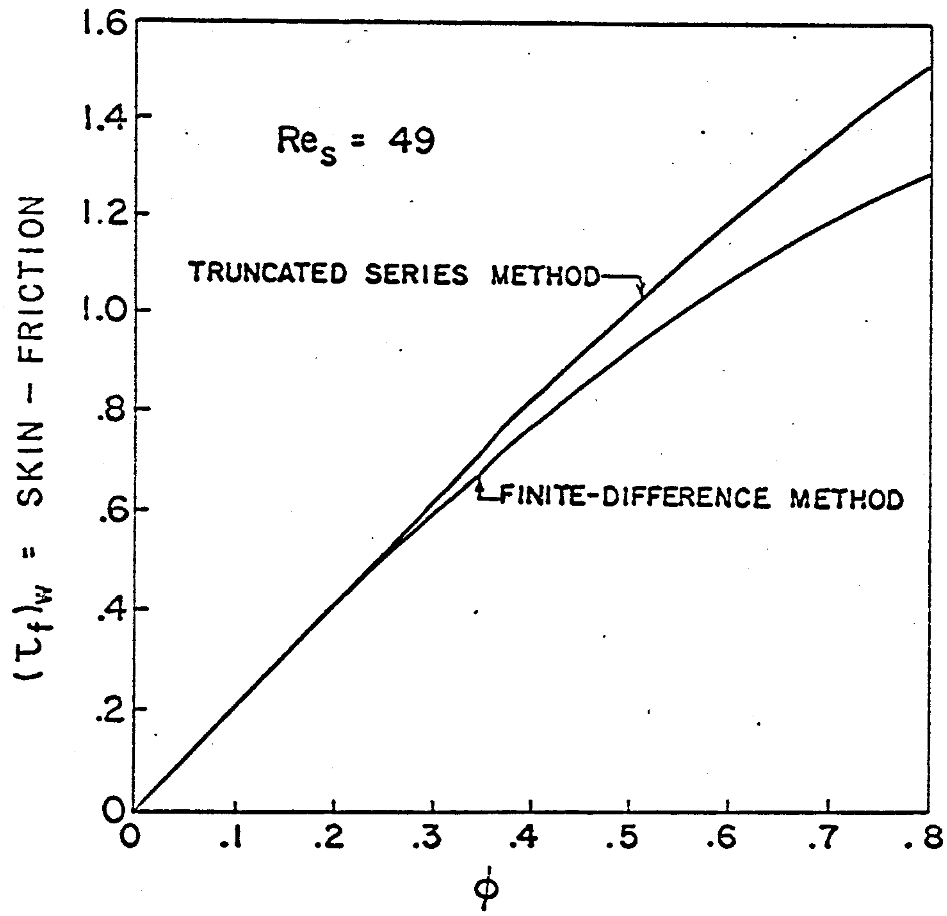

Figure 4a Variation of Skin-Friction for $Re_s = 49$

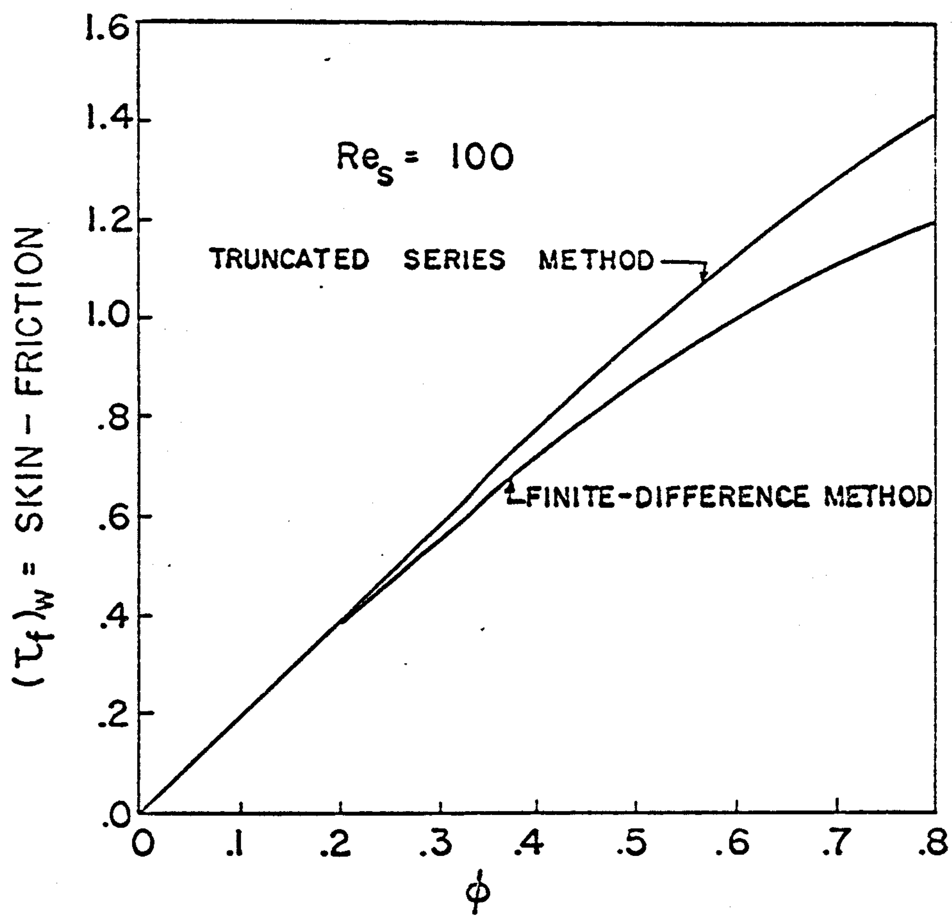

Figure 4b Variation of Skin-Friction for $Re_s = 100$

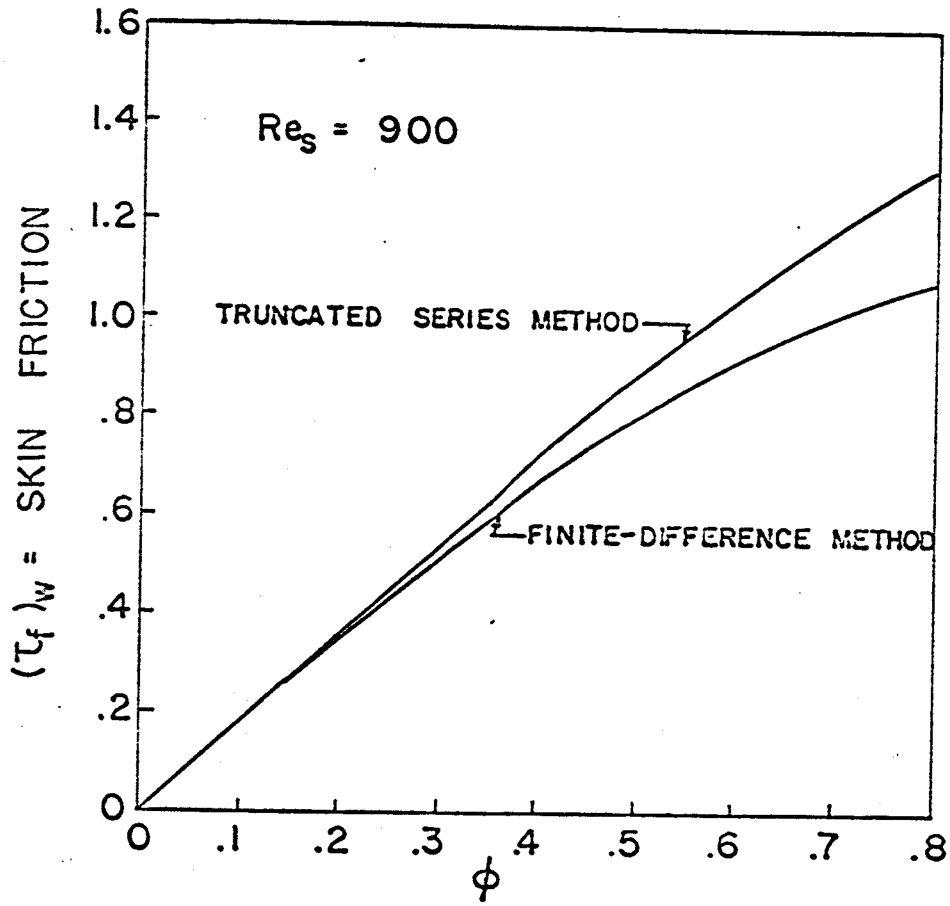

Figure 4c Variation of Skin-Friction for Re_s = 900

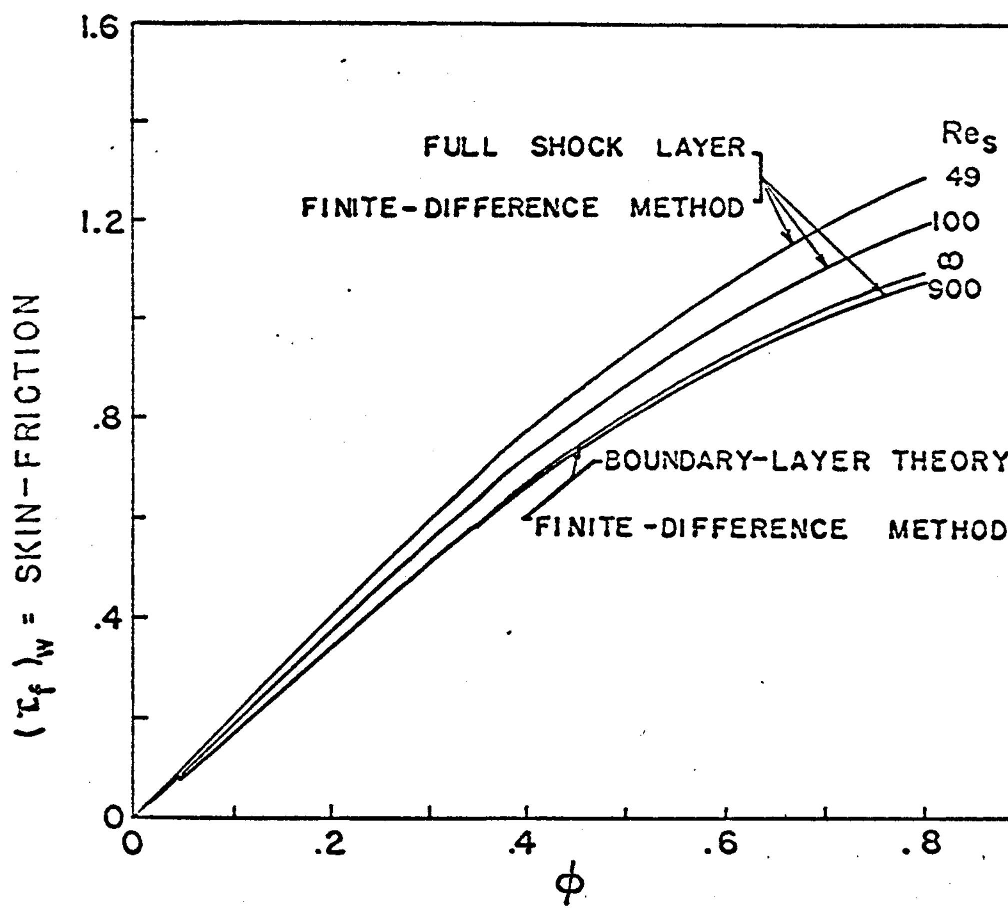

Figure 4d Variation of Skin-Friction at Various Reynolds Numbers

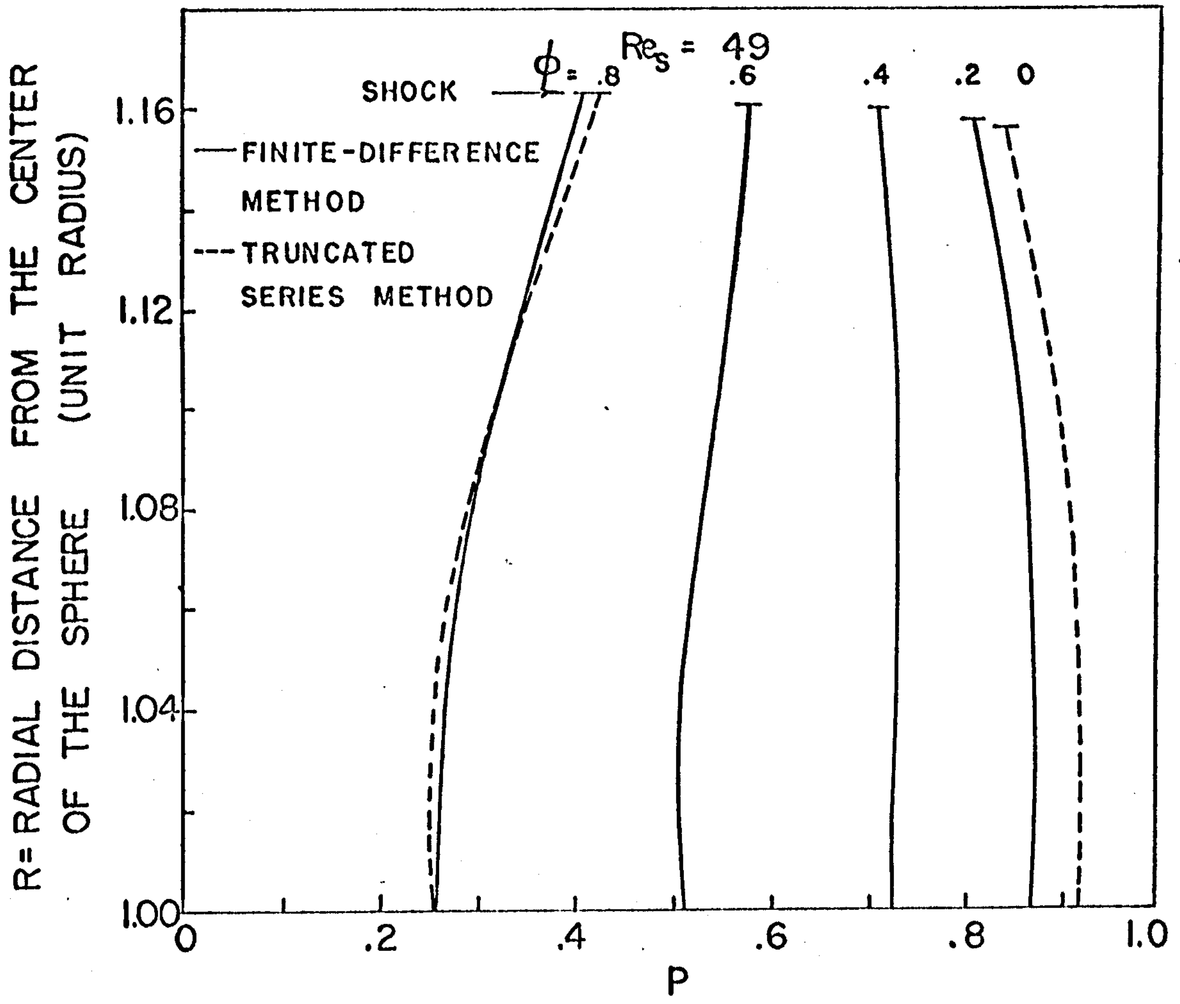

Figure 5a Pressure Distribution for the Flow with $Re_s = 49$

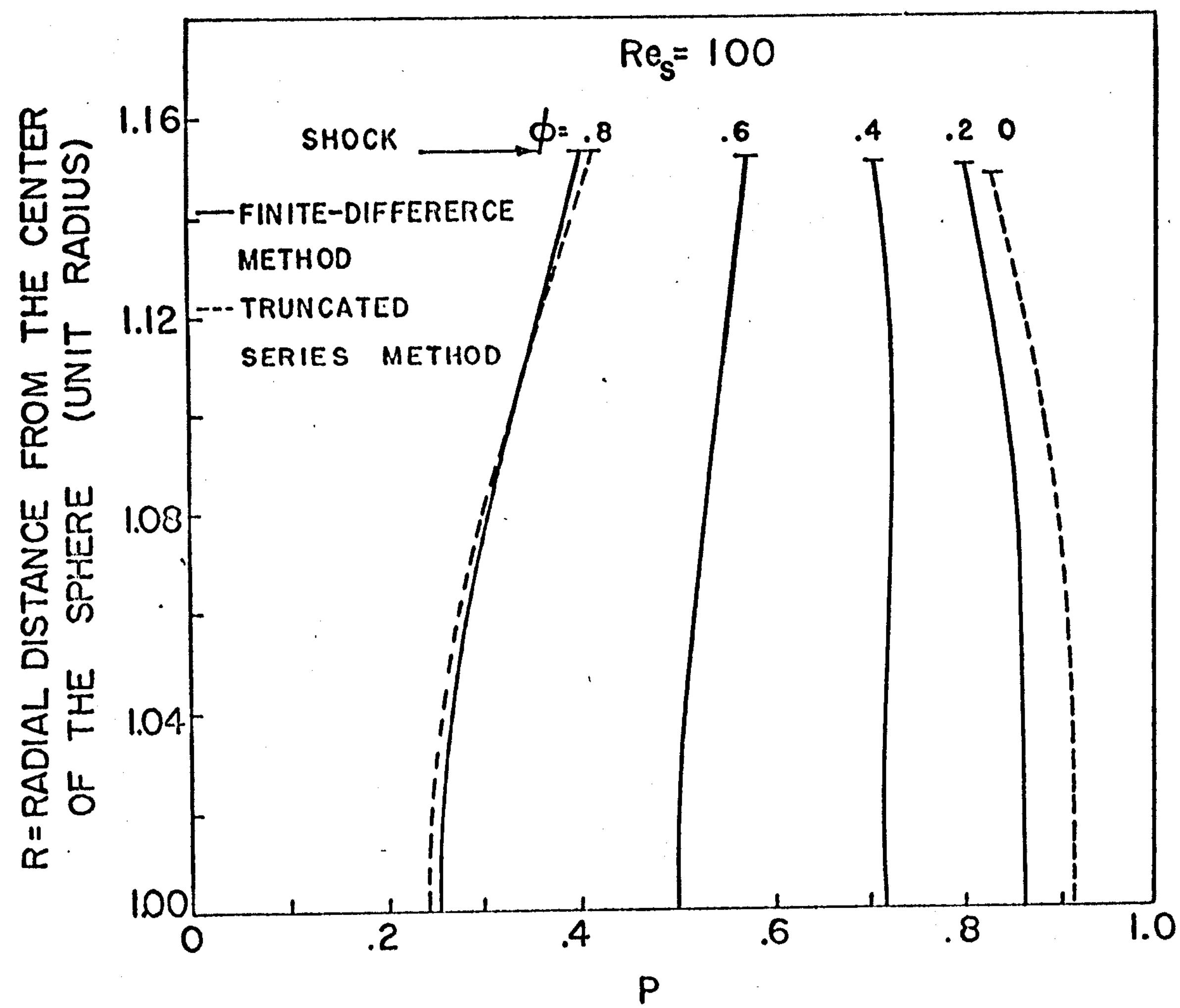

Figure 5b Pressure Distribution for the Flow with Re_s = 100

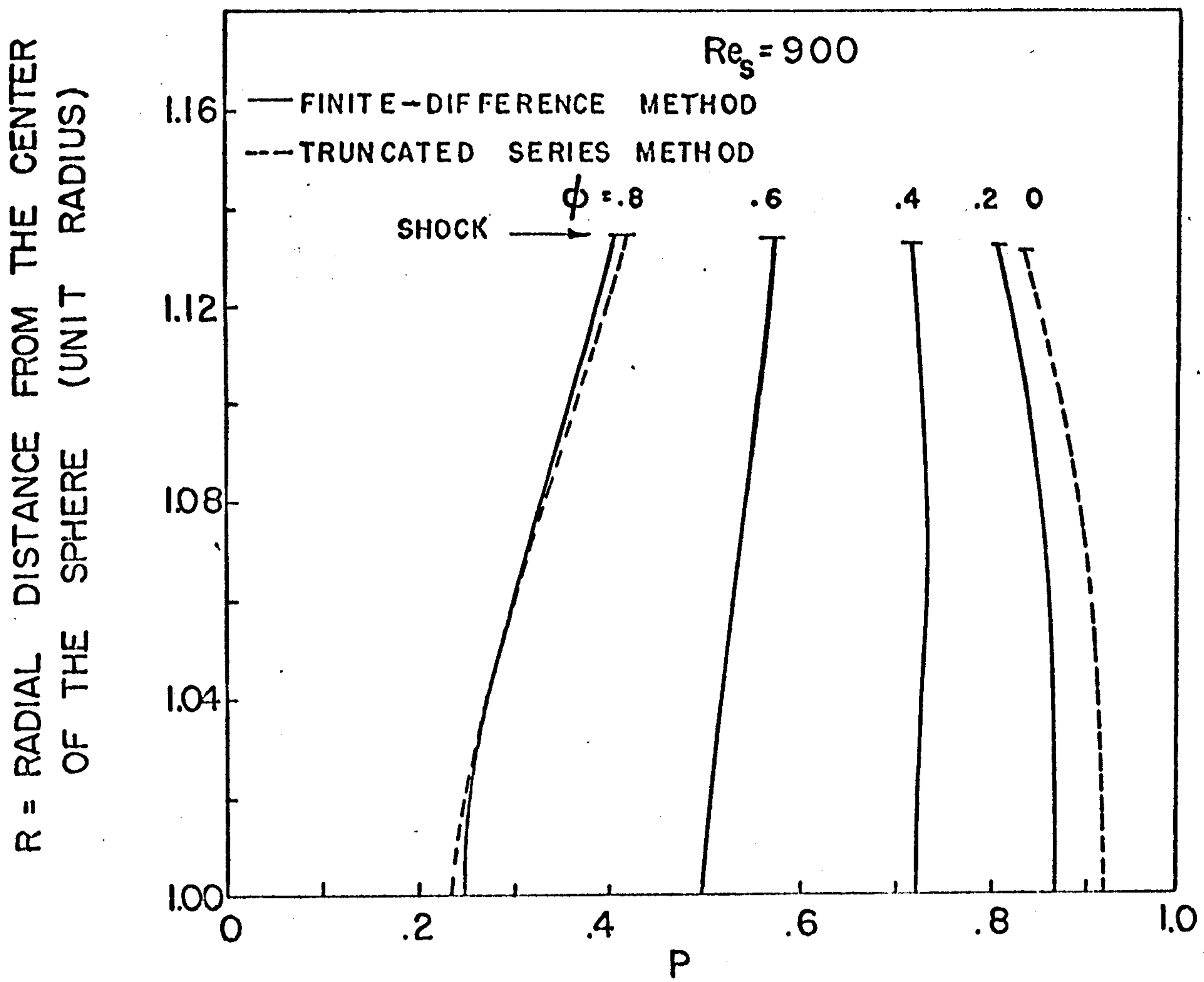

Figure 5c Pressure Distribution for the Flow with Re_s = 900

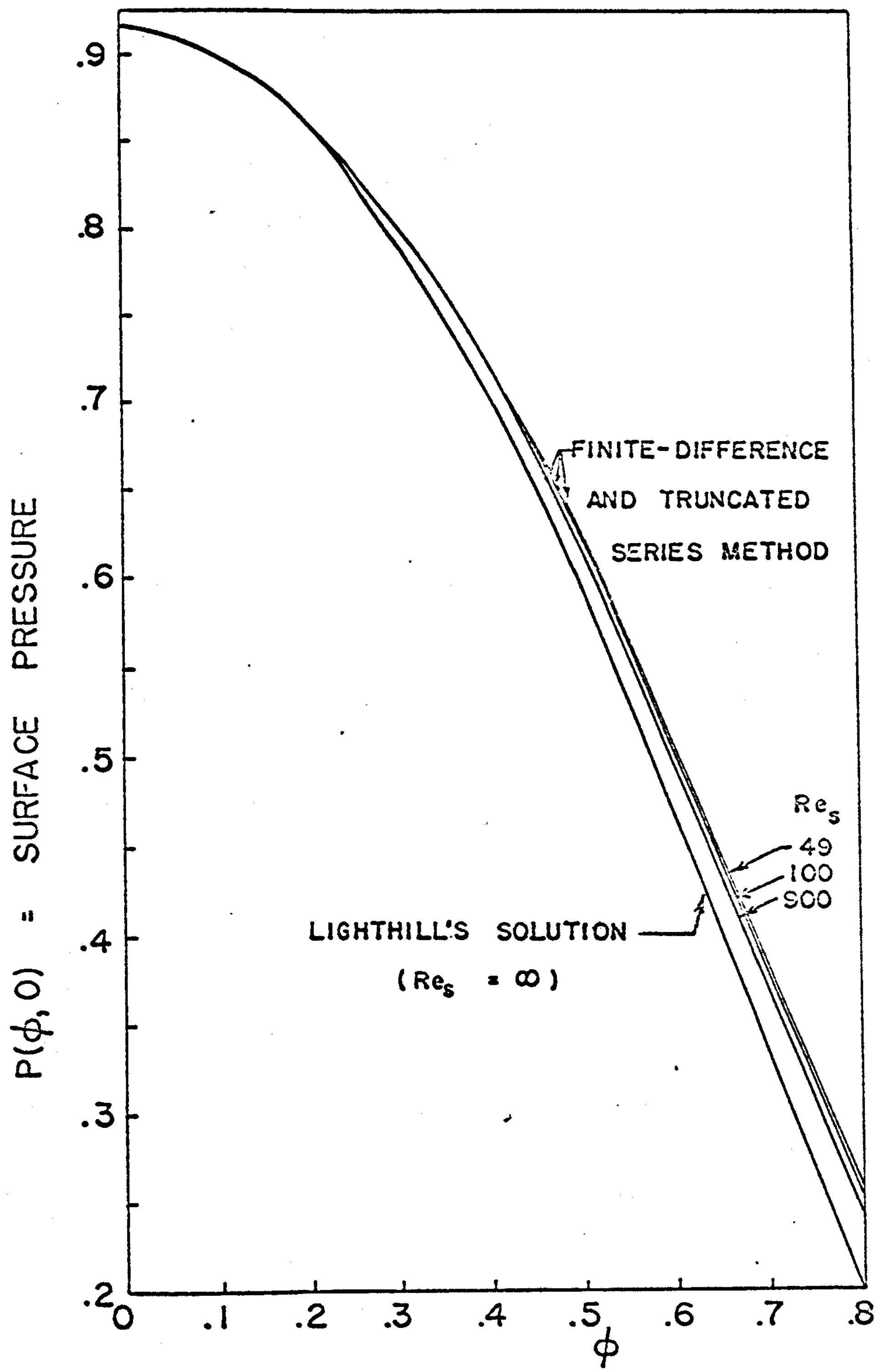

Figure 5d Variation of Surface-Pressure Along the Body Surface for Various Reynolds Numbers